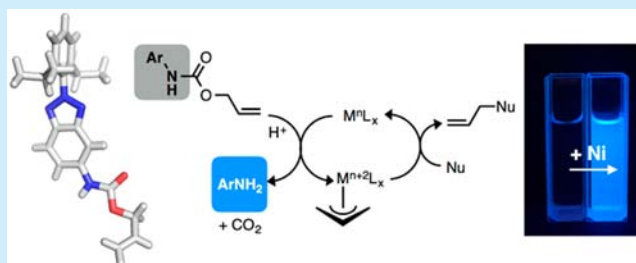


Conformationally Distorted π -Conjugation for Reaction-Based Detection of Nickel: Fluorescence Turn-on by Twist-and-FragmentSeyong Kim,[†] Junyong Jo,[‡] and Dongwhan Lee^{*,†}[†]Department of Chemistry, Seoul National University, 1 Gwanak-ro, Gwanak-gu, Seoul 08826, Korea[‡]Process and Analytical Chemistry, Merck Research Laboratories, 126 East Lincoln Avenue, Rahway, New Jersey 07065, United States

Supporting Information

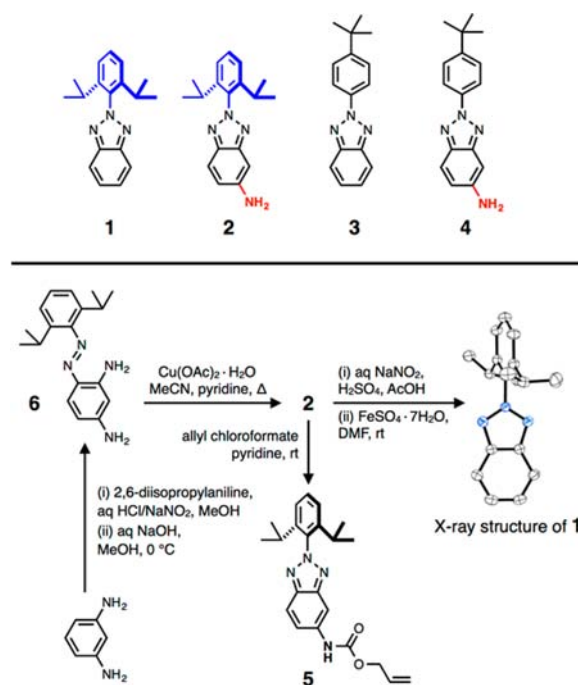
ABSTRACT: A conformationally twisted *N*-arylbenzotriazole was designed as a fluorescence turn-on molecular probe. Under ambient conditions, metal-catalyzed deallylation reactions restore an intense blue emission. This reaction scheme is applicable exclusively to Group 10 transition metal ions and optimized, in particular, for nickel to allow sub-micromolar detection with no competition from other first-row transition-metal ions.



Research on sustainable catalysis with earth-abundant metals is becoming an active area in contemporary chemistry.¹ For quality control in large-scale metal-catalyzed processes, it is imperative to detect residual metal species in the reaction batches in routine fashion.² As a cheap and abundant first-row transition metal, nickel could serve as a surrogate for its rare and expensive (yet much more popularized) congeners, palladium and platinum.³ With an increasing number of nickel-mediated chemical transformations joining the mainstream chemistry,⁴ straightforward detection methods are in need for its high-throughput on-site analysis. Within this context, reaction-based fluorescence turn-on detection of nickel has both conceptual appeal and operational simplicity, but has yet to be realized. We disclose its first example here.

Our entry into this chemistry was prompted by the serendipitous discovery of the rather peculiar light-emitting properties of **1** and **2**, prepared according to Scheme 1. Unlike the prototypical benzotriazole fluorophore **3** ($\lambda_{\text{max,abs}} = 310$ nm; $\lambda_{\text{max,em}} = 430$ nm; fluorescence quantum yield (Φ_F) = 100% in MeCN; $t = 298$ K),⁵ compound **1** is completely nonfluorescent (Figure 1). Both **1** and **3** are built upon the same benzotriazole π -skeleton yet differ by the *N*-aryl substituent. While **3** has a freely rotating *N*-phenyl ring, the bulky 2,6-diisopropyl substituents in **1** enforce an essentially orthogonal arrangement (with torsional angles of 84.7° and 85.9° determined for two chemically equivalent but crystallographically independent molecules in the unit cell) between the *N*-aryl group and the benzotriazole portion of the molecule (Scheme 1, Figure S1).

Intriguingly, installation of an amino group onto the benzotriazole ring of **1** restores the blue emission of the “twisted” *N*-arylbenzotriazole **2** (Figures 1 and S2; $\lambda_{\text{max,em}} = 420$ nm; $\Phi_F = 33\%$ in MeCN; $t = 298$ K),⁶ but its protonated form $[2\cdot\text{H}]^+$ becomes nonfluorescent, just like **1** (Figure 1). In stark contrast, conformationally unconstrained analogues **3** and **4** are both emissive, regardless of the absence/presence of the amino

Scheme 1. Chemical Structures of **1**–**6** and Synthetic Routes

group (Figure S3). Moreover, protonated $[4\cdot\text{H}]^+$ is fluorescent as well ($\lambda_{\text{max,abs}} = 315$ nm; $\lambda_{\text{max,em}} = 380$ nm; $\Phi_F = 46\%$ in MeCN; $t = 298$ K) (Figure S3).

Findings made on **1**–**4** indicate that an interplay between (i) conformational restriction and (ii) covalent modification profoundly impacts the photophysical properties of *N*-

Received: July 20, 2016

Published: August 25, 2016

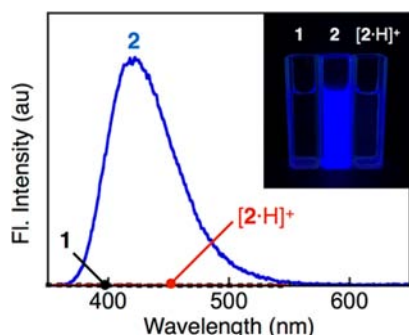
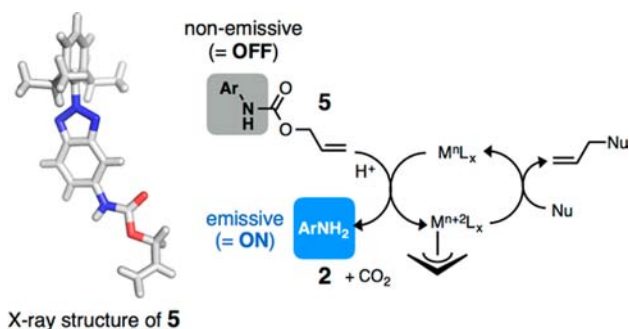


Figure 1. Fluorescence emission spectra of **1** ($\lambda_{\text{exc}} = 280$ nm; black dashed lines), **2** ($\lambda_{\text{exc}} = 335$ nm; blue solid lines), and $[2\cdot\text{H}]^+$ ($\lambda_{\text{exc}} = 280$ nm; red dashed lines) in MeCN (sample concentrations = $20\ \mu\text{M}$) at 298 K. Protonated $[2\cdot\text{H}]^+$ was generated in situ by treating **2** with an excess amount (50 mM) of TFA. Digital images in the inset were obtained with a hand-held UV lamp ($\lambda_{\text{exc}} = 365$ nm).

arylbenzotriazoles. The fluorescence ON–OFF behavior of **2** (Figure 1), in particular, suggests that the availability of amine lone-pair electrons, conjugated directly to the benzotriazole π -system, dictates the emissive properties of the twisted molecule. Without such conformational restriction, optical switching could not be implemented (Figure S3).

In order to turn this empirical observation into useful applications, we prepared compound **5** (Scheme 2; Figure S4) by converting the amino group in **2** to the allyl carbamate functionality (Scheme 1).

Scheme 2. Metal-Catalyzed Deallylation Reaction of **5** as the Signal Transduction Mechanism for Fluorescence Turn-on Detection



This structural engineering resulted in systematic shifts in the excitation/emission profile (Figure S5), so that **5** is essentially nonfluorescent upon excitation at $\lambda_{\text{exc}} = 335$ nm. In contrast, its precursor **2** has the most intense fluorescence when excited at $\lambda_{\text{exc}} = 335$ nm (Figure S6). An important practical implication of this fortuitous situation is that a large enhancement in emission is anticipated to occur upon **5**-to-**2** chemical transformation. Indeed, under standard Tsuji–Trost deallylation conditions using palladium (Scheme 2),⁷ **5** cleanly converts to **2** to elicit a net fluorescence turn-on response (Figure 2a).

In 2007, the Koide group reported reaction-based detection of palladium by deallylation of a “masked” fluorophore.^{11a} Since then, this strategy has widely been implemented with various allyl ethers,⁸ carbamates,⁹ and carbonates;¹⁰ some of these systems also respond to platinum¹¹ or rhodium as well.¹² Our initial studies have shown that the deallylation reaction of **5**

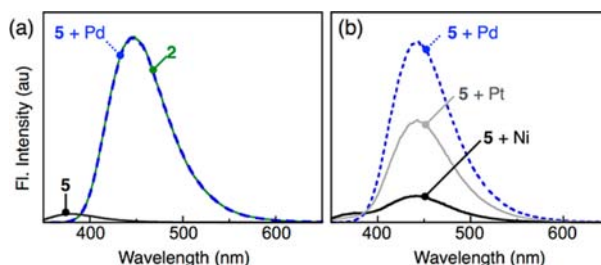


Figure 2. (a) Fluorescence turn-on of **5** ($20\ \mu\text{M}$) in the presence of palladium(II) ion ($10\ \mu\text{M}$) in MeCN/ H_2O (7:3, v/v) containing tri(2-furyl)phosphine (TFP) ($100\ \mu\text{M}$) and NaBH_4 ($100\ \mu\text{M}$). The emission spectrum ($\lambda_{\text{exc}} = 340$ nm; blue dashed lines) of the reaction mixture was taken 5 min after mixing ($t = 298$ K). The overlaid spectrum of **2** (green solid lines; measured independently for a $20\ \mu\text{M}$ solution sample) confirms quantitative formation of **2** by deallylation of **5** (Scheme 2). (b) Fluorescence response of **5** toward different Group 10 metal ions (sample concentrations = $10\ \mu\text{M}$) under the same reaction conditions as in (a).

with palladium(II) (see Figure 2a caption for detailed reaction conditions) is complete within 5 min to quantitatively produce **2** (Scheme 2). This process is accompanied by a large (>150-fold) enhancement in blue emission at $\lambda_{\text{max,em}} = 445$ nm (Figure 2a); formation of **2** as the reaction product was confirmed by HPLC analysis (Figure S7).

Our subsequent studies revealed that **5** responds not only to palladium(II), but also to other Group 10 metals, such as nickel(II) and platinum(II) (Figure 2b). The normalized emission spectra confirmed that these reactions produced the same product, **2**. Under similar conditions, however, other transition metals showed no reactivity (Figure S8) and no interference (Figures S9 and S10).

As Group 10 congeners, palladium and nickel could operate through similar mechanistic manifolds involving d^{10} metal(0) species, generated in situ under reducing conditions to function as a nucleophile (Scheme 2). Indeed, nickel-mediated deallylation protocols are known for allyl ether,¹³ carbamate, and carbonate substrates.¹⁴ This intuitive connection between palladium and nickel chemistry immediately suggested the feasibility of repurposing palladium-responsive systems for reaction-based fluorescence turn-on detection of nickel, for which no literature examples exist.

Toward this objective, we have screened various combinations of solvents, ligands, reducing equivalents, and reagent concentrations to maximize the conversion of **5** to **2** using nickel(II). Unlike palladium-catalyzed deallylation, electron-rich $\text{P}(p\text{-Tol})_3$ or PPh_3 performed better than electron-deficient TFP or $\text{P}(4\text{-FPh})_3$ (Figure 3a), although they are sterically comparable (cone angle = 133° for TFP;¹⁵ 145° for $\text{P}(4\text{-FPh})_3$,¹⁶ $\text{P}(p\text{-Tol})_3$,¹⁷ and PPh_3 ¹⁸).

Under optimized reaction conditions (see Figure 3a caption for details), > 90% conversion was achieved within 15 min at 25°C , with > 120-fold enhancement in the fluorescence intensity at $\lambda_{\text{max,em}} = 450$ nm, and visually detectable blue emission of the deallylation product **2** (Figure 3b). The high sensitivity of **5** under this condition allows for sub-micromolar-level detection of nickel(II). A plot of $I_{450\text{ nm}}$ vs metal concentration shows a linear relationship down to the value of $[\text{Ni}^{2+}] = 100\ \text{nM}$ (Figure S11). Formation of **2** in the reaction was confirmed by HPLC analysis as well (Figure S12).

Among the first-row transition metals that we have screened, this fluorescence turn-on reaction manifold (Scheme 2) works

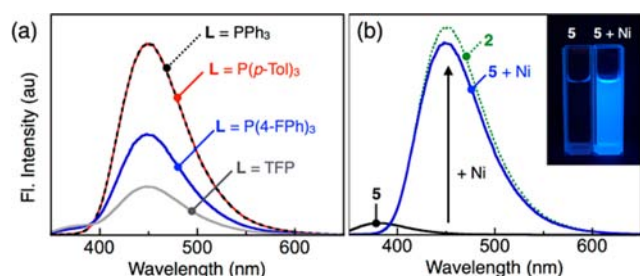


Figure 3. (a) Reactivity screening by fluorescence ($\lambda_{\text{exc}} = 340$ nm) enhancement from the reaction between **5** (20 μM) and nickel(II) (10 μM) in MeCN/H₂O (3:7, v/v) containing phosphine ligands (200 μM) and NaBH₄ (200 μM). Each reaction was stirred for 15 min at $t = 298$ K before measurement. (b) Nickel-triggered deallylation of **5** to produce **2** as fluorescence turn-on signal. Under the reaction conditions described for (a), PPh₃ was used as the ligand. Inset: digital images obtained under a hand-held UV lamp ($\lambda_{\text{exc}} = 365$ nm).

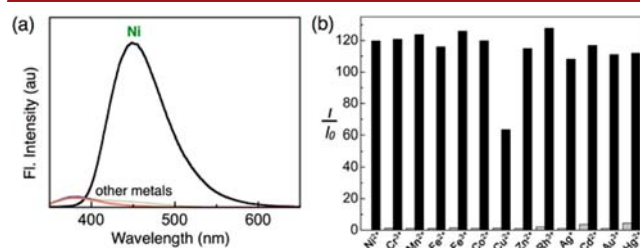


Figure 4. (a) Fluorescence response ($\lambda_{\text{exc}} = 340$ nm) of **5** (20 μM) toward nickel(II) and various transition-metal ions (10 μM ; see the list in (b)) in MeCN/H₂O (3:7, v/v) containing PPh₃ (200 μM) and NaBH₄ (200 μM). Each reaction mixture was stirred for 15 min at $t = 298$ K before measurement was made. (b) Selectivity of **5** for nickel(II) over other transition-metal ions under the reaction conditions described for (a). Gray bars: fluorescence response toward metal ions. Black bars: fluorescence response for nickel(II) in the presence of other metal ions. I : fluorescence intensity at $\lambda = 450$ nm. I_0 : fluorescence intensity of the probe-only sample at $\lambda = 450$ nm.

exclusively for nickel (Figure 4), with no or little interference observed when equimolar mixtures of nickel and other metals were allowed to compete.¹⁹ The reactivity is maintained consistently across various nickel(II) sources of different counteranions (AcO[−], Cl[−], NO₃[−], and SO₄^{2−}; Figure S13), thus ruling out the involvement of trace metal contaminants in the response pattern that we observe.

Under the conditions that work best for nickel, its heavier Group 10 congeners palladium and platinum also elicit turn-on response (Figure S14). The reactivity pattern (Ni > Pt > Pd), however, is entirely reversed compared to the conditions developed initially for palladium (Pd > Pt > Ni; Figure 2b). Reaction optimization is thus key to our success in fluorescence turn-on detection of nickel. In retrospect, this seems to be the most logical next step beyond the already mature palladium-detection methodology. We could only speculate why no intentional efforts seem to have been made in this direction before.

While cheap and earth-abundant metals are less susceptible to supply fluctuations, controlling the level of such elementary impurities poses a significant challenge in fine chemicals industry. In fact, the regulatory requirements are becoming increasingly difficult to meet, necessitating rigorous and iterative purification and analytical processes. Nickel is a Class 1 metal, which is defined as metals of significant safety

concerns by the European Medicines Agency (EMA).²⁰ Biological and environmental toxicity of nickel is also well-known.²¹ As a human carcinogen, the exposure limit of nickel in the active pharmaceutical ingredient (API) is 2.5 ppm for parenteral exposure and as low as 100 ng/day for inhalation exposure.²²

Previous efforts have employed ligand-appended fluorophores²³ or chromophores²⁴ to detect nickel(II). Such chelation-based strategy, however, often suffers from interference with other first-row metal ions,²⁵ in particular, copper(II).²⁶ A higher binding affinity of copper(II) toward what is designed to be a nickel(II) binding site²⁷ often leads to complete fluorescence quenching.²⁸ As an alternative, a reaction-based fluorescence detection scheme should suffer less from such limitations but has not been realized before.

To the best of our knowledge, compound **5** represents the first example of reaction-based fluorescence turn-on probe for nickel. For process control in which the concoction of each reaction batch is already known and the detection of trace metal is important, this approach should have the largest impact. Efforts are currently underway in our laboratory to improve on the sensitivity as well as spectral window of this first-generation prototype.

■ ASSOCIATED CONTENT

Supporting Information

The Supporting Information is available free of charge on the ACS Publications website at DOI: 10.1021/acs.orglett.6b02140.

Synthesis and characterization of **1**, **2**, **5**, and **6**; additional spectroscopic, chromatographic, and X-ray crystallographic data (PDF)
X-ray data for **1** (CIF)

■ AUTHOR INFORMATION

Corresponding Author

*E-mail: dongwhan@snu.ac.kr.

Notes

The authors declare no competing financial interest.

■ ACKNOWLEDGMENTS

This work was supported by the National Research Foundation of Korea (NRF Grant No. 2014R1A2A2A01002650) and BK21 PLUS Fellowship (to S.K.).

■ REFERENCES

- (1) (a) Su, B.; Cao, Z.-C.; Shi, Z.-J. *Acc. Chem. Res.* **2015**, *48*, 886–896. (b) Gandeepan, P.; Cheng, C.-H. *Acc. Chem. Res.* **2015**, *48*, 1194–1206. (c) Morris, R. H. *Acc. Chem. Res.* **2015**, *48*, 1494–1502. (d) Holland, P. L. *Acc. Chem. Res.* **2015**, *48*, 1696–1702. (e) Liu, W.; Groves, J. T. *Acc. Chem. Res.* **2015**, *48*, 1727–1735. (f) McCann, S. D.; Stahl, S. S. *Acc. Chem. Res.* **2015**, *48*, 1756–1766. (g) Zell, T.; Milstein, D. *Acc. Chem. Res.* **2015**, *48*, 1979–1994. (h) McNeill, E.; Ritter, T. *Acc. Chem. Res.* **2015**, *48*, 2330–2343. (i) Ryken, S. A.; Schafer, L. L. *Acc. Chem. Res.* **2015**, *48*, 2576–2586. (j) Li, Y.-Y.; Yu, S.-L.; Shen, W.-Y.; Gao, J.-X. *Acc. Chem. Res.* **2015**, *48*, 2587–2598. (k) Oloo, W. M.; Que, L., Jr. *Acc. Chem. Res.* **2015**, *48*, 2612–2621.
- (2) (a) Jiang, P.; Guo, Z. *Coord. Chem. Rev.* **2004**, *248*, 205–229. (b) Formica, M.; Fusi, V.; Giorgi, L.; Micheloni, M. *Coord. Chem. Rev.* **2012**, *256*, 170–192. (c) Sahoo, S. K.; Sharma, D.; Bera, R. K.; Crisponi, G.; Callan, J. F. *Chem. Soc. Rev.* **2012**, *41*, 7195–7227. (d) Carter, K. P.; Young, A. M.; Palmer, A. E. *Chem. Rev.* **2014**, *114*,

- 4564–4601. (e) Zhu, H.; Fan, J.; Wang, B.; Peng, X. *Chem. Soc. Rev.* **2015**, *44*, 4337–4366.
- (3) (a) Yamaguchi, J.; Muto, K.; Itami, K. *Eur. J. Org. Chem.* **2013**, 2013, 19–30. (b) Han, F.-S. *Chem. Soc. Rev.* **2013**, *42*, 5270–5298. (c) Montgomery, J. *Organonickel Chemistry*. In *Organometallics in Synthesis*, 4th ed.; Lipshutz, B. H., Ed.; John Wiley & Sons, Inc.: Hoboken, 2013; pp 319–428. (d) Tobisu, M.; Chatani, N. *Acc. Chem. Res.* **2015**, *48*, 1717–1726. (e) Tollefson, E. J.; Hanna, L. E.; Jarvo, E. R. *Acc. Chem. Res.* **2015**, *48*, 2344–2353.
- (4) (a) Rosen, B. M.; Quasdorf, K. W.; Wilson, D. A.; Zhang, N.; Resmerita, A.-M.; Garg, N. K.; Percec, V. *Chem. Rev.* **2011**, *111*, 1346–1416. (b) Hu, X. *Chem. Sci.* **2011**, *2*, 1867–1886. (c) Tasker, S. Z.; Standley, E. A.; Jamison, T. F. *Nature* **2014**, *509*, 299–309. (d) Ananikov, V. P. *ACS Catal.* **2015**, *5*, 1964–1971.
- (5) Jo, J.; Lee, H. Y.; Liu, W.; Olasz, A.; Chen, C.-H.; Lee, D. J. *Am. Chem. Soc.* **2012**, *134*, 16000–16007.
- (6) With increasing solvent polarity, **2** displays red-shifted emission (Figure S2), which implicates the involvement of CT-type excited states.
- (7) (a) Tsuji, J.; Takahashi, H.; Morikawa, M. *Tetrahedron Lett.* **1965**, *6*, 4387–4388. (b) Trost, B. M.; Fullerton, T. J. *J. Am. Chem. Soc.* **1973**, *95*, 292–294. (c) Guibé, F. *Tetrahedron* **1998**, *54*, 2967–3042. (d) Weissman, S. A.; Zewge, D. *Tetrahedron* **2005**, *61*, 7833–7863.
- (8) (a) Garner, A. L.; Song, F.; Koide, K. *J. Am. Chem. Soc.* **2009**, *131*, 5163–5171. (b) Kitley, W. R.; Santa Maria, P. J.; Cloyd, R. A.; Wysocki, L. M. *Chem. Commun.* **2015**, *51*, 8520–8523. (c) Nie, H.; Geng, J.; Jing, J.; Li, Y.; Yang, W.; Zhang, X. *RSC Adv.* **2015**, *5*, 97121–97126. (d) Koide, K.; Tracey, M. P.; Bu, X.; Jo, J.; Williams, M. J.; Welch, C. J. *Nat. Commun.* **2016**, *7*, 10691.
- (9) (a) Jiang, J.; Jiang, H.; Liu, W.; Tang, X.; Zhou, X.; Liu, W.; Liu, R. *Org. Lett.* **2011**, *13*, 4922–4925. (b) Baker, M. S.; Phillips, S. T. *J. Am. Chem. Soc.* **2011**, *133*, 5170–5173. (c) Zhang, L.; Wang, Y.; Yu, J.; Zhang, G.; Cai, X.; Wu, Y.; Wang, L. *Tetrahedron Lett.* **2013**, *54*, 4019–4022.
- (10) Chen, X.; Li, H.; Jin, L.; Yin, B. *Tetrahedron Lett.* **2014**, *55*, 2537–2540.
- (11) (a) Song, F.; Garner, A. L.; Koide, K. *J. Am. Chem. Soc.* **2007**, *129*, 12354–12355. (b) Garner, A. L.; Koide, K. *Chem. Commun.* **2009**, 83–85. (c) Garner, A. L.; Koide, K. *Chem. Commun.* **2009**, 86–88.
- (12) Song, F.; Carder, E. J.; Kohler, C. C.; Koide, K. *Chem. - Eur. J.* **2010**, *16*, 13500–13508.
- (13) Taniguchi, T.; Ogasawara, K. *Angew. Chem., Int. Ed.* **1998**, *37*, 1136–1137.
- (14) Corey, E. J.; Suggs, W. J. *Org. Chem.* **1973**, *38*, 3223–3224.
- (15) Andersen, N. G.; Keay, B. A. *Chem. Rev.* **2001**, *101*, 997–1030.
- (16) Clavier, H.; Nolan, S. P. *Chem. Commun.* **2010**, *46*, 841–861.
- (17) Tolman, C. A. *Chem. Rev.* **1977**, *77*, 313–348.
- (18) Tolman, C. A. *J. Am. Chem. Soc.* **1970**, *92*, 2956–2965.
- (19) The only exception is copper(II), for which a somewhat diminished fluorescence was observed. A mixture of **2** and copper(II), prepared independently to simulate the reaction conditions, does not show any change in the emission intensity, thus ruling out fluorescence quenching of the reaction product (by the paramagnetic metal species) as the main reason for this behavior.
- (20) EMA Guidelines: Specification Limits for Residues of Metal Catalysts or Metal Reagents. http://www.ema.europa.eu/ema/index.jsp?curl=pages/regulation/general/general_content_000737.jsp&mid=WC0b01ac0580028e8c (accessed Jun 22, 2016).
- (21) (a) Denkhaus, E.; Salnikow, K. *Crit. Rev. Oncol. Hemat.* **2002**, *42*, 35–56. (b) Klein, C.; Costa, M. Nickel. In *Handbook on the Toxicology of Metals*, 4th ed.; Nordberg, G. F.; Fowler, B. A.; Nordberg, M., Eds.; Elsevier: London, 2015; pp 1091–1111.
- (22) ICH Quality Guidelines: Q3D Guideline for Elemental Impurities. <http://www.ich.org/products/guidelines/quality/article/quality-guidelines.html> (accessed Jun 22, 2016).
- (23) (a) Kavitha, R.; Stalin, T. *J. Lumin.* **2015**, *158*, 313–321. (b) Ganjali, M. R.; Hosseini, M.; Motalebi, M.; Sedaghat, M.; Mizani, F.; Faridbod, F.; Norouzi, P. *Spectrochim. Acta, Part A* **2015**, *140*, 283–
287. (c) Annaraj, B.; Mitu, L.; Neelakantan, M. A. *J. Mol. Struct.* **2016**, *1104*, 1–6.
- (24) (a) Goswami, S.; Chakraborty, S.; Paul, S.; Halder, S.; Maity, A. C. *Tetrahedron Lett.* **2013**, *54*, 5075–5077. (b) Liu, X.; Lin, Q.; Wei, T.-B.; Zhang, Y.-M. *New J. Chem.* **2014**, *38*, 1418–1423. (c) Goswami, S.; Chakraborty, S.; Das, A. K.; Manna, A.; Bhattacharyya, A.; Quah, C. K.; Fun, H.-K. *RSC Adv.* **2014**, *4*, 20922–20926.
- (25) (a) Abebe, F. A.; Eribal, C. S.; Ramakrishna, G.; Sinn, E. *Tetrahedron Lett.* **2011**, *52*, 5554–5558. (b) Li, H.; Zhang, S.-J.; Gong, C.-L.; Li, Y.-F.; Liang, Y.; Qi, Z.-G.; Chen, S. *Analyst* **2013**, *138*, 7090–7093. (c) Biswas, S.; Acharyya, S.; Sarkar, D.; Gharami, S.; Mondal, T. K. *Spectrochim. Acta, Part A* **2016**, *159*, 157–162.
- (26) (a) Fabbri, L.; Licchelli, M.; Pallavicini, P.; Perotti, A.; Sacchi, D. *Angew. Chem., Int. Ed. Engl.* **1994**, *33*, 1975–1977. (b) Fabbri, L.; Licchelli, M.; Pallavicini, P.; Perotti, A.; Taglietti, A.; Sacchi, D. *Chem. - Eur. J.* **1996**, *2*, 75–82. (c) Bolletta, F.; Costa, I.; Fabbri, L.; Licchelli, M.; Montalti, M.; Pallavicini, P.; Prodi, L.; Zaccaroni, N. *J. Chem. Soc., Dalton Trans.* **1999**, 1381–1385. (d) Fabbri, L.; Licchelli, M.; Parodi, L.; Poggi, A.; Taglietti, A. *Eur. J. Inorg. Chem.* **1999**, 1999, 35–39. (e) Ros-Lis, J. V.; Martínez-Máñez, R.; Soto, J.; McDonagh, C.; Guckian, A. *Eur. J. Inorg. Chem.* **2006**, 2006, 2647–2655. (f) Kaur, N.; Kumar, S. *Chem. Commun.* **2007**, 3069–3070. (g) Banerjee, A.; Sahana, A.; Guha, S.; Lohar, S.; Hauli, I.; Mukhopadhyay, S. K.; Matalobos, J. S.; Das, D. *Inorg. Chem.* **2012**, *51*, 5699–5704. (h) Li, Z.; Zhao, W.; Li, X.; Zhu, Y.; Liu, C.; Wang, L.; Yu, M.; Wei, L.; Tang, M.; Zhang, H. *Inorg. Chem.* **2012**, *51*, 12444–12449. (i) Zhang, L.; Wang, Y.; Wan, C.; Xing, Z.; Li, W.; Li, M.; Zhang, S. X.-A. *RSC Adv.* **2015**, *5*, 66416–66419.
- (27) (a) Irving, H.; Williams, R. J. P. *Nature* **1948**, *162*, 746–747. (b) Irving, H.; Williams, R. J. P. *J. Chem. Soc.* **1953**, 3192–3210.
- (28) (a) Dodani, S. C.; He, Q.; Chang, C. J. *J. Am. Chem. Soc.* **2009**, *131*, 18020–18021. (b) Kang, M. Y.; Lim, C. S.; Kim, H. S.; Seo, E. W.; Kim, H. M.; Kwon, O.; Cho, B. R. *Chem. - Eur. J.* **2012**, *18*, 1953–1960.